Int J Adv Manuf Technol
DOI 10.1007/s00170-016-9017-2

ORIGINAL ARTICLE

Effect of tool geometry on mechanical behavior of friction stir spot welds of polycarbonate sheets

F. Lambiase[1,2] · **A. Paoletti**[1,2] · **A. Di Ilio**[1,2]

Received: 20 April 2016 / Accepted: 6 June 2016

Abstract This study investigates the influence of the tool dimensions on the mechanical behavior of friction stir spot welds performed on polycarbonate sheets. Different tools were used by varying the pin geometry (cylindrical and tapered) and the diameters of the tool pin and that of the tool shoulder. Morphological analysis was conducted to determine the extension of the welded zone and main defects of the welds. Single lap shear tests were carried out to determine the influence of the tool dimension on the mechanical behavior of the welds. The onset and evolution of failure during the shear tests was analyzed. Five different failure modes were identified which showed both a brittle and ductile behavior. According to the achieved results, the strength of the welds reduced with increasing the pin diameter and taper angle. On the other hand, the strength increased with increasing the tool shoulder diameter. However, the highest specific strength, calculated as the ratio of the shear strength by the tool area, reduced with increasing the shoulder diameter. Under the optimal processing conditions, the strength of the joints reached up to 88 % of the shear strength of the base material.

Keywords Friction spot stir welding · Polymers · Welding · Single lap shear test · Mechanical behavior · Shear strength

✉ F. Lambiase
francesco.lambiase@univaq.it

[1] Department of Industrial and Information Engineering and Economics, University of L'Aquila, via G. Gronchi 18, Zona Industriale di Pile, L'Aquila 67100 (AQ), Italy

[2] University of Naples Federico II, CIRTIBS Research Centre, P.le Tecchio 80, 80125 Naples, Italy

1 Introduction

Polymeric materials as well as reinforced polymers are increasingly employed in the production of lightweight components to reduce the vehicle weight, fuel consumption, and consequently the overall product performances. In this context, the connection of subparts represents a key issue since here it usually develops stress concentration (owing to static or dynamic load) as well as corrosion phenomena. Joining different materials involves additional limitations concerning the suitable joining technology to use. Thus, several processes have been developed in the recent years to overcome the main limitations of conventional welding, mechanical joining, and adhesive bonding technologies.

Combined thermo-mechanical processes such as friction lap welding [1, 2], friction spot welding [3–8], and friction-based stacking [9, 10] have been demonstrated to be suitable for joining polymers, reinforced polymers, and hybrid structures comprising metal parts.

Besides the above-mentioned ones, friction stir-based (FSB) processes such as friction stir welding (FSW) and friction spot stir welding (FSSW) have been successfully employed to join different types of polymers including high-density polyethylene (HDPE) [11–14], polycarbonate (PC) [15–18], polyethylene (PE) [19–23], acrylonitrile butadiene styrene (ABS) [14, 24–28], polymethylmethacrylate (PMMA) [28, 29], polyamide (PA) [30–32], and (PP) [33–37]. The growing interest in these processes is due to the ability to join materials with different thermal and physical properties, restrict the heating region, which leads to higher efficiency and reduced heat-affected zone, produce low thermal distortions, and produce joints with mechanical behavior being comparable to other welding processes [7] often close to the strength of the base material. In addition, FSW and FSSW offer further advantages over competitive processes such as

Published online: 11 June 2016

low equipment investments, requirement of lower energy, and easy automation [25].

Although a large number of investigations have been carried out on FSW and FSSW of metal parts, a fewer studies have concerned with FSB processes of polymers. However, since the high difference in terms of thermal, rheological, and mechanical properties between metals and thermoplastic polymers, specific studies are required to select the proper processing conditions and improve the quality of welds made by FSW and FSSW [28] on polymeric materials. So far, the scientific literature has principally focused on three main aspects: analysis and optimization of the tool geometry, optimization of the processing conditions, and development of new type of tools.

The characteristics dimensions of the FSW tool, namely, the pin diameter, the tool shoulder, and the taper angle influence the heat generated and the material flow; thus, they influence the defects occurrence and weld dimension and finally the weld strength [38] and the elongation at break. Being based on the material stirring, the influence of the pin geometry on the mechanical strength of the welds is of primary importance and it has been deeply investigated in [23]. In addition, the overall dimension of the tool, which includes both the tool pin and the tool shoulder, also influences the loads and energy involved in FSSW especially during the plunging phase (when the material is relatively cold and the contact forces reach the highest values) [15].

The weld strength is determined by the stirring quality, the upsetting exerted by the tool shoulder, and the temperature distribution in the welding region. The heat supplied during the welding depends on the combination of the processing conditions namely the tool rotational speed, the feed rate and the tilt angle in FSW and the tool rotational speed, the plunging speed, the pre-heating time, and the stirring time in FSSW. A number of investigations have been performed to determine the influence of the processing conditions on the mechanical behavior of the welds produced by the FSB processes. The weld strength increases by increasing the tool rotation speeds then it reaches a maximum and then it decreases [19, 30]. Under low values of tool rotation speed, under-heating conditions develop leading to poor material mixing. On the other hand, if the excessive heat is supplied (e.g., increasing the tool rotation speed or reducing the feed rate), the material undergoes high softening resulting in the reduction of the friction generated and the upsetting load [16]. Both of these conditions are detrimental for the welds strength.

Since FSB processes involve complex interactions among the process parameters, tool dimensions, material characteristics, and structured and robust optimization techniques based on artificial neural network [17] on either statistical approach [22, 39] have been involved to determine the optimal processing conditions.

A number of modifications to the basic process have been introduced to improve the weld quality achieved by FSW and FSSW processes. The control of the plunging force would be beneficial to reduce the variation of the plunging force during the welding process due to variation of the tool-material contact force [27]. The adhesion between the materials can be strengthened by introducing multi-walled carbon nanotubes (MWCNTs) at the interface of the sheets [11, 13].

The improvement of the mechanical behavior of these welds has been pursued also by the development of new type of tools. FSW and FSSW produce welds with a V-shaped profile, which results in a weak mechanical behavior of the weld in correspondence of the pin (back slit effect). To this end, tools with two shoulders named "self-retracting tool" have been introduced to eliminate back slit effect [24]. In FSB processes, the tool shoulder exerts an upsetting action on the material extruded vertically from the pin region. However, if the tool shoulder rotates with the tool pin, the extruded material is ejected from the weld. In addition, because of the great frictional work between the tool shoulder and the underlying material, high increase in local temperature is observed causing material softening and reduction in the axial pressure. Furthermore, because of the low thermal conductivity of polymers, high thermal gradients develop between the stirring region and the base material (which is slightly heated) leading to weak welds. A possible solution is represented by the employment of tools with rotating pins but fixed shoulders. Such tools, which have been generally employed for the FSW process, are often coupled with heating and temperature control systems to keep constant the tool shoulder temperature during the welding process [12]. As a result, higher quality and more standardized welds are produced [21, 40]. The improvement in the weld quality is due to a better stirring of the material [29] other than lower variation of the axial force during FSW [41].

So far, any study has been conducted to evaluate the influence of the tool dimensions during friction stir spot welding of polymer sheets. In addition, a few details have been reported in literature concerning the fracture development of such welds. Thus, the current investigation aimed at understanding the influence of the tool dimensions in friction spot stir welding of polycarbonate sheets. An experimental campaign was carried out using different tools varying the tool pin geometry (cylindrical or tapered), the pin, and the shoulder diameters. Geometrical characterization of the welds was carried out by means of optical microscopy and the influence of the tool geometry on the dimension of the welded zone was investigated. Single lap shear test were carried out to determine the mechanical behavior of the welds. Finally, fractography analysis was performed to relate the mechanical properties of the welds to their geometrical characteristics.

2 Materials and methods

2.1 Experimental setup

Thin sheets with 3.0 mm of thickness made of polycarbonate (PC) were used during the experimental campaign. Polycarbonate is an amorphous thermoplastic with a wide range of applications in different industrial fields such as optical industry, automotive, and household applications owing to good optical transparency, high strength and toughness. The material is characterized by glass transition temperature $T_g = 147$ °C, and it shows high elongation at break of 110 % and tensile strength of 60 MPa [18].

Friction stir spot welds were performed by a CNC drilling machine. The machine is controlled by an electronic IO system connected to common PC. To address the influence of the tool geometry, ten different tools were involved by varying: the tool pin geometry cylindrical ($\alpha = 0°$) or tapered ($\alpha = 30°$), the pin diameter ($d = 5$, 10 mm), and the shoulder diameter ($D = 10$, 15, and 20 mm). The tool dimensions are reported in Table 1. The tool identifier was composed of two numbers: the first is a progressive identifier of the pin and shoulder dimension, while the second indicates the taper angle. The tools were made of K340 stainless steel, which is a heat treatable steel, turned under a CNC turning machine.

Before each welding experiment, the tool was cooled down at room temperature (such a temperature was measured by means of by a pyrometer type 1060–2 connected to Thermophil INFRA type 4472 thermometer) and cleaned from material which remained attached to the pin. The FSSW tests were performed under displacement control. Each test started by putting in rotation the tool at a prescribed speed n, and it was slightly plunged within the material (with a depth of 0.1 mm) for a prescribed time T_p; then, the tool continued to plunge the material with a constant speed v_f as long as a given plunging depth (s) was reached. Thus, the plunging motion was stopped (begin of the stirring time) while the tool rotation continued. As the prescribed dwell time T_D was elapsed, the tool rotation was also stopped to enable the material cooling for the prescribed waiting time T_W; then, the tool was retracted from the weld.

The processing parameters such as the plunging speed ($v_f = 8$ mm/min), the pre-heating time ($T_p = 7$ s), the dwell time ($T_D = 21$ s), the waiting time ($T_W = 21$ s), and the tool rotational speed ($n = 1260$ rpm) were kept constant at optimal values found in [42].

2.2 Characterization of FSSW welds

Single lap shear tests were performed in order to assess the mechanical behavior of the welds. A schematic of the specimen is reported in Fig. 1. The shear tests were carried out using a universal MTS 322.31 testing machine with 25 kN full-scale load at a constant cross-head speed of 0.5 mm/min. Five replicates were performed for each testing condition. The shear strength F_r, calculated as the maximum load during the test, and the specific strength S_s, calculated as the ratio of the shear strength by the tool shoulder area:

$$S_s = \frac{F_r}{\pi \cdot (D/2)^2} \quad (1)$$

and the absorbed energy E were recorded during each single lap shear test.

Further tests were performed on sectioned specimens. During these tests, pictures of the cross section were taken to investigate the deformation of the welds and the crack propagation path. To this end, a 16-bit DSLR camera model D5200 by Nikon with a resolution of 6000 × 4000 was used in combination with macro lens (×10). An external trigger with a timer was used to acquire one picture per second.

Optical microscopy analysis was carried out to characterize the welds dimension and to better investigate the type of fracture. To this end, the welds were sectioned using a precision cutting rotary blade and subsequently polished up to 1200 paper grit and polishing compounds for polymeric materials. Then, fractography analysis was performed by means of a digital microscope model KH-8700 by Hirox.

3 Results and discussion

3.1 Morphological analysis and critical dimensions of the welds

A typical cross section of a friction stir spot weld is reported in Fig. 2. The macrograph shows the keyhole left by the tool pin after the process, which is common to this type of weld. The FSS weld is characterized by a compact region (CR) without porosities close to the side surface of the keyhole owing to the high temperature produced during the stirring phase and compressive stress developing during the consolidation phases. When polymers are welded by friction spot stir welding, high

Table 1 Main dimensions of adopted tools

Tool ID	1-0	2-0	3-0	4-0	5-0	1-30	2-30	3-30	4-30	5-30
Pin diameter, d [mm]	5	10	5	10	5	5	10	5	10	5
Shoulder diameter, D [mm]	20	20	15	15	10	20	20	15	15	10
Taper angle, α [deg]	0	0	0	0	0	30	30	30	30	30

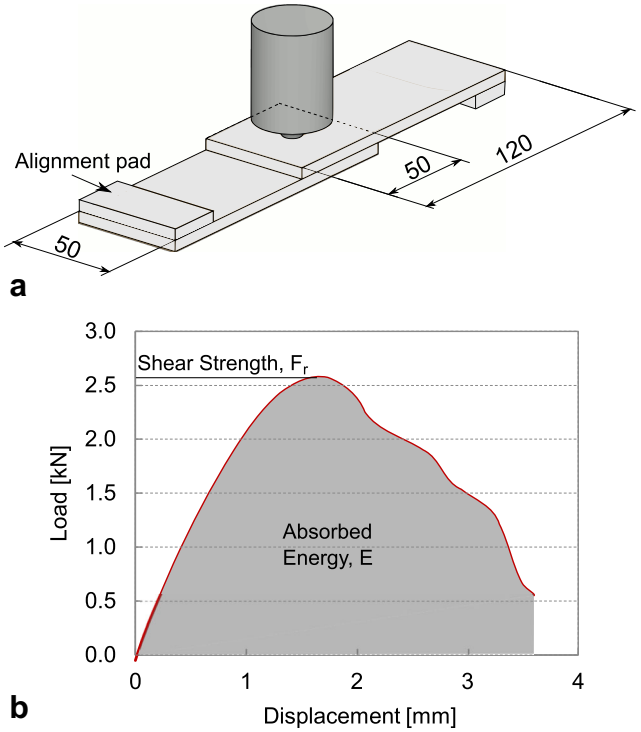

Fig. 1 **a** Schematic of shear test specimen and **b** mechanical characteristics of FSS welds during shear tests

temperature gradients are produced between the stirred zone and the substrate (whose temperature increase is negligible) since the low thermal conductivity of such materials. Thus, a high number of porosities may develop at the interface leading to a poor adhesion. As a result, a porous zone (PZ) may develop between the CR and the base material (BM). The porosities may act as stress raiser during loading conditions and thus they may determine a drastic reduction in the mechanical performances of the weld. From the macrograph, it is also evident that the welded region is more extended than the porous zone, since the presence of a transparent (welded) ring surrounding the PZ.

The development of the above-mentioned defects depends on the selection of the process conditions. Actually, in friction stir welding of polymers, high levels of heat (resulting from high tool rotation speed and low transverse speed) allowed to reduce or even avoid the development of such defects [27]. Decreasing the tool rotation speed induces the formation of many cavities since the heat generated is insufficient to establish the bonding of material plastically deformed by the tool. On the other hand, the presence of porosities is mainly related to the air entrapped in the weld owing to insufficient material flow. In FSSW of polymers, the occurrence of porosities can be also induced by the thermal shrinkage, trapped air, or even structural changes of the polymer [7].

Therefore, the proper selection of the tool and plunging depth is aimed at reducing the presence of the above-mentioned defects but also increasing all the critical weld dimensions, which influence the fracture, namely, the welded area A_{weld}, the interface area between the stirred zone and the upper sheet A_{up} and the interface area of the stirred zone with the lower sheet A_{lo}, reported in Fig. 3. A reduced welded area A_{weld} facilitates the development of shear fracture in the weld region; on the other hand, the welds showing low values of A_{up} or A_{lo} will fail by separation of the stirred zone from the upper and lower sheet, respectively.

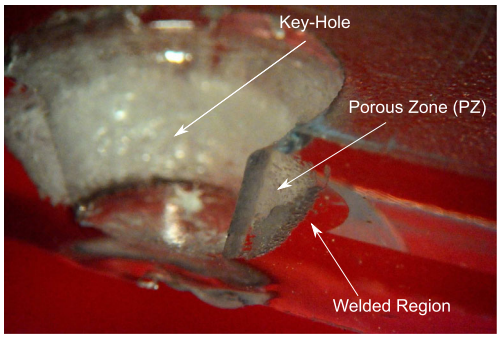

Fig. 2 Cross section of a FSSW showing the characteristics regions ($d=5$ mm, $D=10$ mm and $a=30°$)

3.2 Effect of the plunging depth

Preliminary experiments were carried out by varying the plunging depth (s) in order to improve the mechanical strength of the weld. The tests were performed using the tool with $d=5$ mm, $D=20$ mm, and $\alpha=0°$. The plunging determines the geometrical characteristics of the welds and consequently their mechanical performances. Increasing the plunging depth s is expected to increase the welded area A_{weld} since more heat is produced near the sheets interface, increase A_{lo} and reduce A_{up}, as depicted in Fig. 4.

Thus, different values of plunging depths were tested including a slightly negative value ($s=-0.08$ mm). Figure 5 depicts the cross sections of welds performed with different values of the plunging depth. As can be inferred, when the tool shoulder plunges the upper sheet ($s>0$) the profile of the stirred zone is very similar regardless the plunging depth. However, as above-mentioned, the welded zone moves towards the lower sheet with the increase in s resulting in the variation of the critical areas A_{up}, A_{lo}, and A_{weld}.

The variation of these critical areas is reported in Fig. 6. Here, the values of the welds performed with $s=-0.08$ are not reported since, as also shown in Fig. 5, the stirred zone was not recognizable. From Fig. 6, it is evident that, A_{up} reduces for $s<0.56$ mm moderately, then for $s=0.66$ mm it reduces more evidently. This is due to the shape of the stirred zone. On the other hand, A_{lo} and A_{weld} increase almost linearly with s for $s<0.56$ mm; then, for $s=0.66$ mm, they benefit of a steep increase since a large part of the stirred zone is within the lower sheet, as shown in Fig. 5.

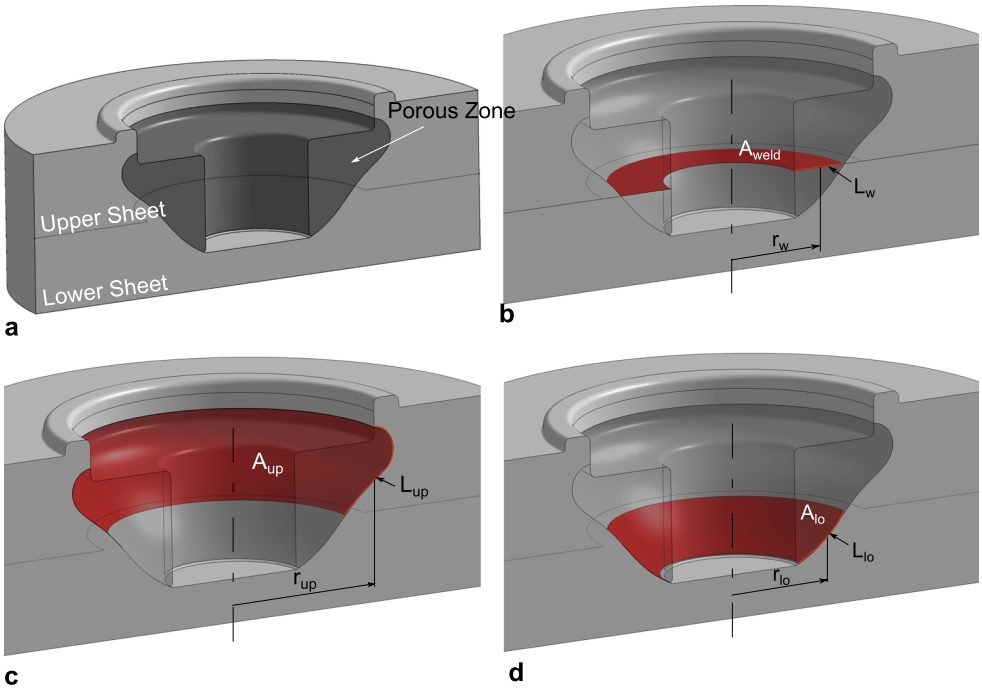

Fig. 3 Critical regions of FSSW of polymers

Figure 7 compares the load-displacement curves of welds performed using different values of s. As can be inferred, the optimal value of the plunging depth was $s = 0.47$ mm. For $s < 0.47$ mm, the welds failed by separation of the stirred zone (SZ) from the lower sheet; thus, L_{lo} (and consequently A_{lo}) was the critical parameter. On the other hand, for $s = 0.47$, $s = 0.56$, and $s = 0.66$ mm the welds failed by separation of the stirred zone from the upper sheet. When $s > 0.47$ mm, the increase in the plunging depth determined an excessive reduction of L_{up} (and A_{up}), resulting in a reduction of the weld strength.

The mechanical characteristics of FSS welds varying the plunging depth s were also summarized in Table 2.

The determination of the optimal tool plunge depth depends on several factors including the sheet thickness and material as well as the disposition of the sheets, when joints are performed on different materials or sheets of different thickness. Furthermore, since the welds failure may happen at the sheets interface with the welding zone, the presence of porosities and cavities and the extension of the stirred zone may also influence the optimal tool plunge depth. Thus, also the tool geometry and the processing conditions including the pressure exerted during the consolidation phase may influence the optimal tool plunge depth. However, the value of the plunging depth $s = 0.47$ mm was kept constant over the performed experiments.

3.3 Failure modes

The mechanical performances of the FSSW welds depend on several factors including the characteristic dimensions of the weld, the presence, distribution, and dimension of voids and porosities, and the shape of the welded zone, which may facilitate the development of stress concentration. During the

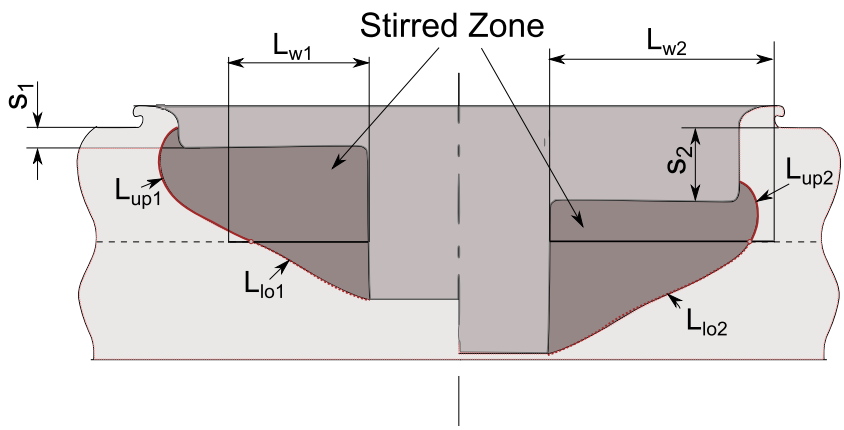

Fig. 4 Effect of plunging depth on geometry of the weld

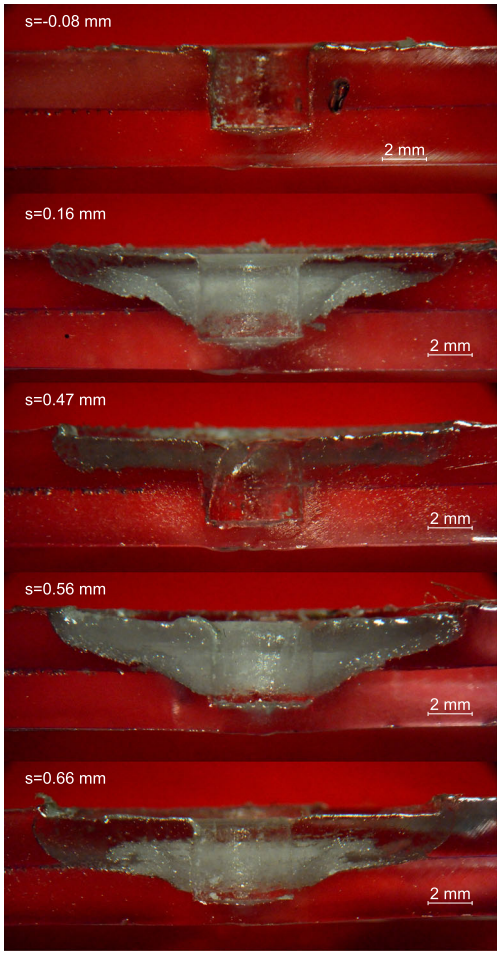

Fig. 5 Effect of plunging depth (*s*) on welds cross sections

single lap shear tests different failure modes were identified, namely brittle fracture in the upper (M1) or lower sheet (M2), separation of the stirred zone from the lower sheet (M3), separation of the stirred zone from the upper sheet (M4), and shear fracture in the welded region (M5).

Brittle fracture was found in the welds made by tools P1-0 and P2-0. These tools are characterized by the larger shoulder

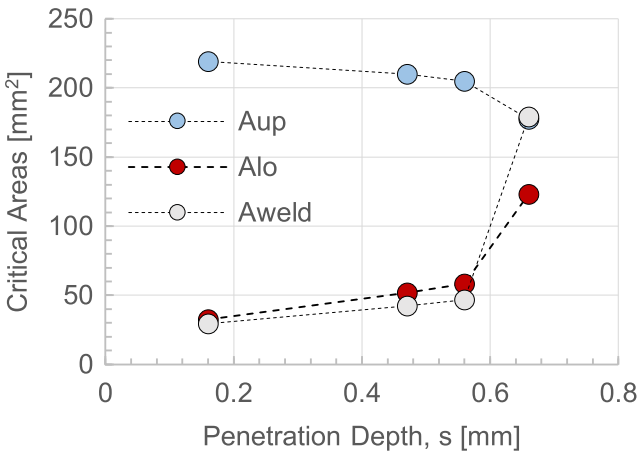

Fig. 6 Effect of plunging depth on the critical areas A_{up}, A_{lo}, and A_{weld}

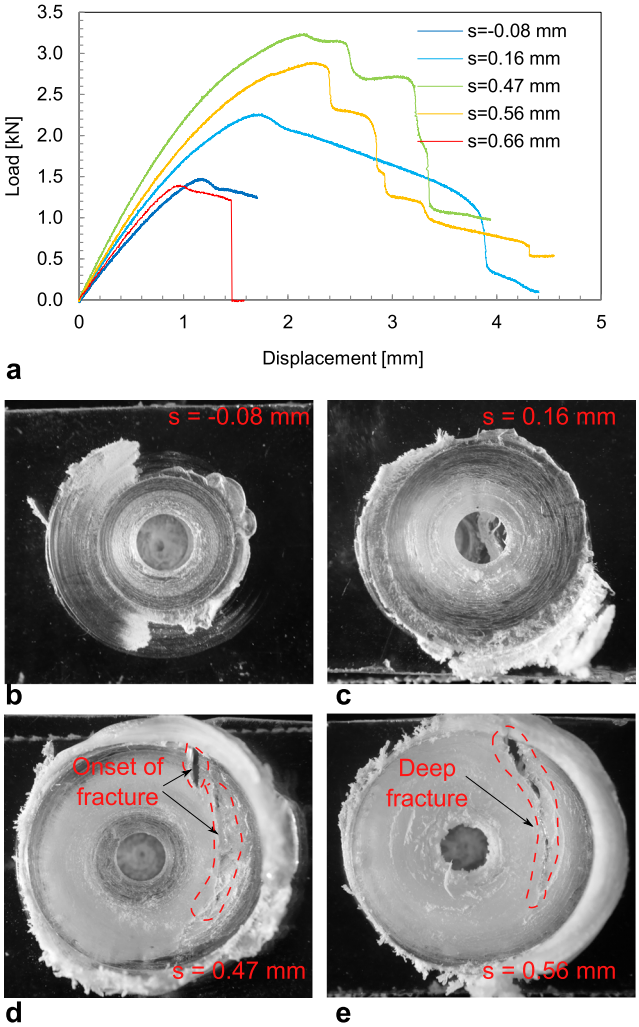

Fig. 7 Influence of the plunging depth (*s*) on the mechanical behavior of the welds during single lap shear tests

diameter ($D = 20$ mm). The fracture developed almost instantly from the onset of the load peak leading to a low absorbed energy but also the highest shear strength. These welds showed a good adhesion between the stirred zone and the substrate. Here, the material reaches a critical stress value that is lower than the yield strength of the base material owing to the presence of the porosities and the residual stress developing during the

Table 2 Mechanical characteristics of FSS welds varying the plunging depth

s [mm]	Shear strength, F_r [kN]	Absorbed energy, E [J]	Specific strength [MPa]
−0.08	1.50	1.70	4.78
0.16	2.27	6.20	7.23
0.47	3.24	8.39	10.32
0.56	2.89	7.14	9.20
0.66	1.40	1.60	4.46

consolidation phase (cooling) and the high temperature gradients. The brittle behavior of such rupture is evident from the fracture surfaces in the upper and lower sheets (Fig. 8a, b).

Figure 9 a, b shows a FSS weld failed by separation of the stirred zone from the lower sheet. This type of weld is characterized by a poor adhesion of the SZ with the substrate owing to the small value of A_{lo}. The porosities within the PZ reduce the effective contact surface and further act as stress raised during shear tests. In such welds, the fracture starts from the point P and proceeds along the interface of stirred zone and lower sheet until the complete separation of these regions, as shown in Fig. 10b.

Figure 9 c, d shows a specimen failed by separation of the stirred zone from the upper sheet. These welds are characterized by good adhesion of the SZ with the lower sheet while poor adhesion of the SZ with the upper sheet owing to a small value of A_{up}. In these welds, the fracture starts from the point P, propagates along the stirred zone-upper sheet interface, and terminates in the upper sheet.

The welds made by tools P4 and P5 (with both $\alpha = 0°$ and $\alpha = 30°$) failed by shear fracture in the welded zone, as shown in Fig. 9 e, f. These welds are characterized by a thin welded area A_{weld} because of the small area under the tool shoulder A_s.

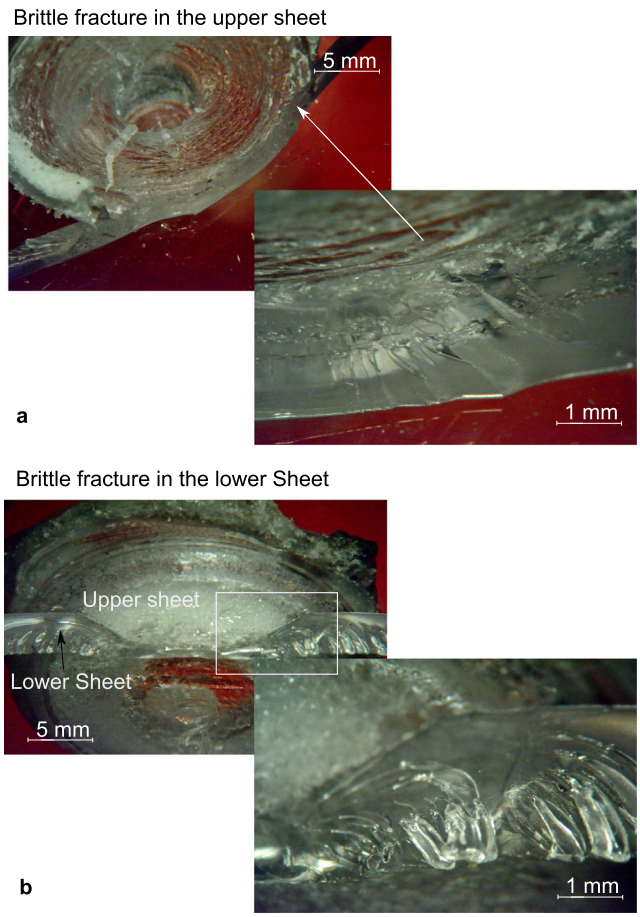

Fig. 8 Macrographs of brittle fracture modes developing in FSSW welds

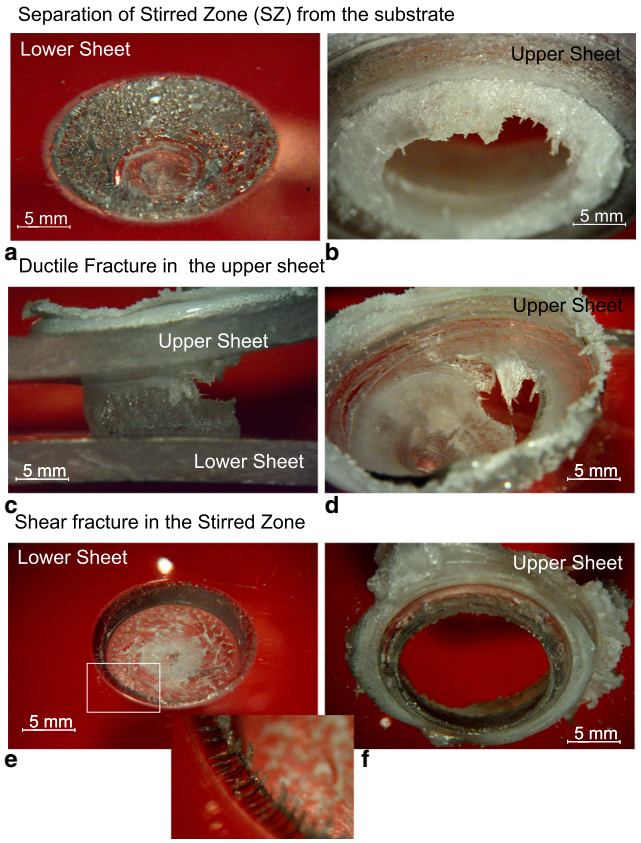

Fig. 9 Macrographs of ductile fracture modes developing in FSSW welds

In these welds, the fracture starts from the point P and propagates along the weld line.

The fracture development of ductile fracture modes M3, M4, and M5 is also depicted in Fig. 11.

3.4 Mechanical behavior of the FSSW welds

Figure 12 compares the shear strength of welds made by tools having cylindrical ($\alpha = 0°$) and tapered ($\alpha = 30°$) pins. The influence of α on the shear strength of the welds made by the tools P1, P2, and P3 is negligible. On the other hand, the shear strength decreases with α in the welds made by the tools P4 and P5. Indeed, these welds are characterized by a small area under the tool shoulder A_s, which is given by Eq. 2:

$$A_s = \pi \cdot \left(\left(\frac{D}{2} \right)^2 - \left(\frac{d}{2} + h_t \cdot sin\alpha \right)^2 \right) \quad (2)$$

where h_t is the tool pin height ($h_t = 4.3$ mm). Thus, the employment of the tapered pins further reduces the dimension of the area A_s and consequently the welded area A_{weld}, leading to a reduction of the shear strength. These results are in slight contrast with the experimental findings reported in [23].

Figure 13a, b summarizes the influence of the tool pin diameter (d) and the shoulder diameter (D) on the shear

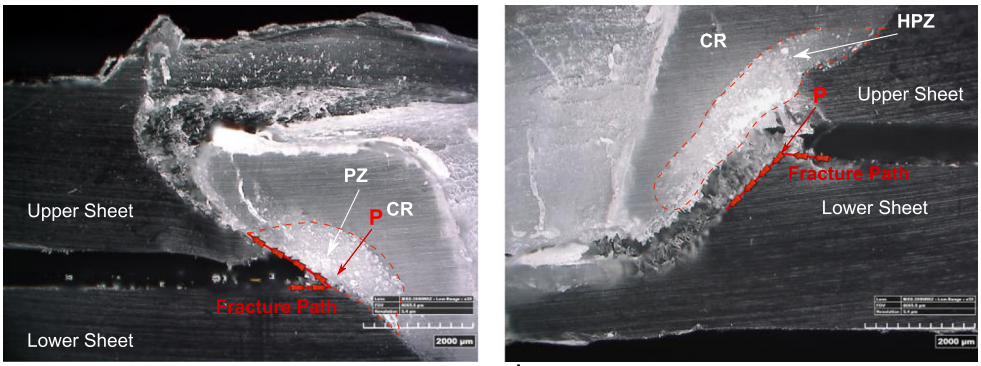

Fig. 10 Fracture Paths: separation of SZ from **a** upper sheet, M4 and **b** lower sheet, M3

strength F_r of the welds. F_r increases with the tool shoulder diameter D, regardless the value of the pin diameter either the taper angle α. Indeed, increasing D comes with the increase of A_{weld} other than higher supplied heating (since greater

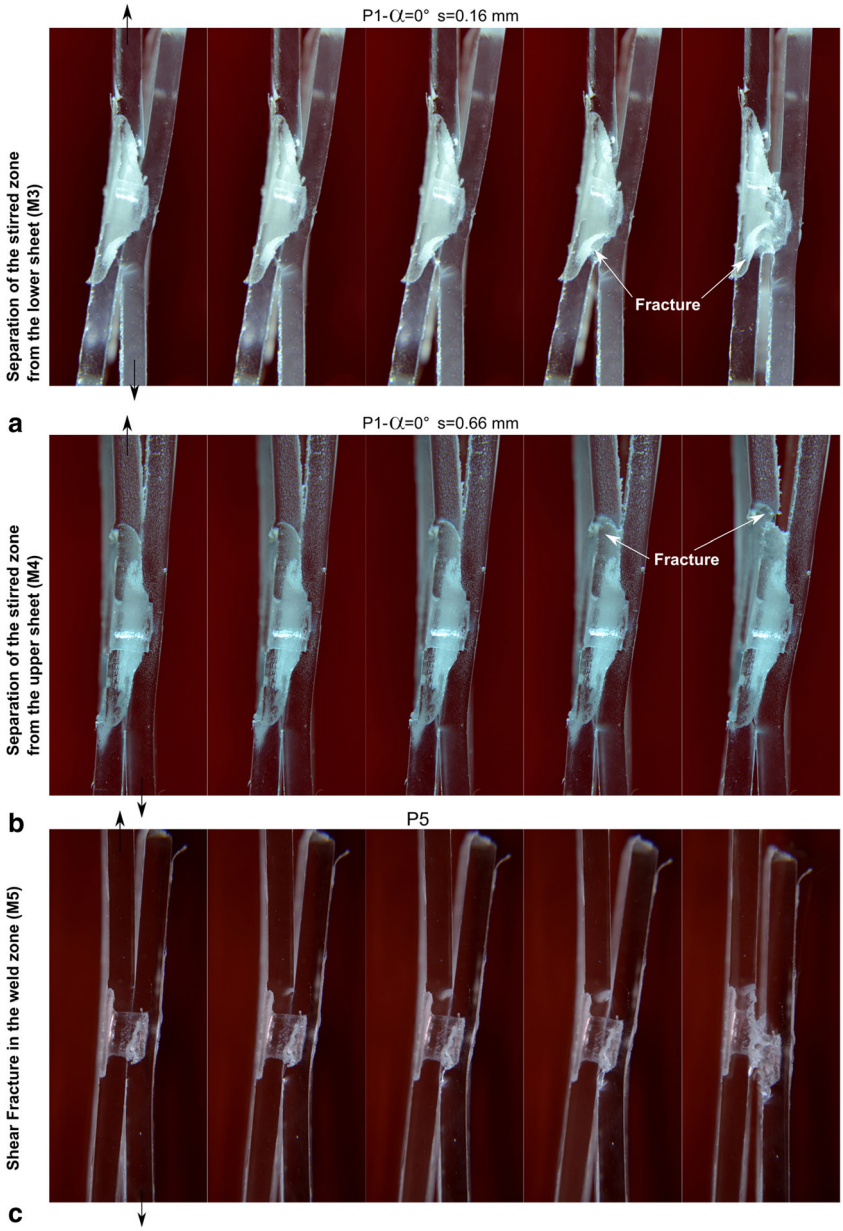

Fig. 11 Fracture development in **a** lower sheet, **b** upper sheet, and **c** weld zone

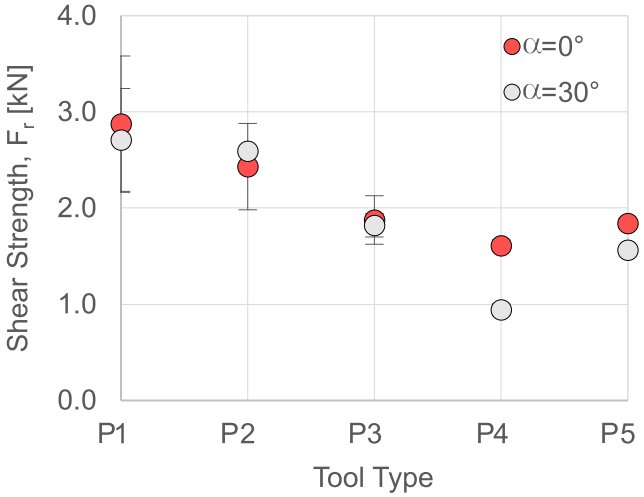

Fig. 12 Effect of the tool geometry on the shear strength of the welds

tangential speed is reached). The welds characterized by the smallest A_{weld} (those produced with tools P4-0, P4-30, P5-0, and P5-30), failed by shear fracture. However, when the tools with the largest shoulder ($D = 20$ mm) were adopted, different fracture modes were observed using the same tool leading to a higher uncertainty on the mechanical behavior of the weld. Such uncertainty, which concerned both shear strength and the absorbed energy, is also confirmed by the increase in the standard deviation values.

The increase in the tool pin diameter comes with a reduction in the shear strength. A larger pin diameter involves higher heating supplied to the weld (since the greater radial velocity); nevertheless, it also results in a larger keyhole and consequently a reduction in the welded area. The reduction of the shear strength with the pin diameter indicates that the effect of the reduction in the welded area is predominant over the increase in the produced heating.

In order to encompass with different fracture modes and compare the mechanical strength of the welds having different dimensions, the specific strength, calculated by Eq. 2, was used. To this end, the geometrical characterization of the welds was done by analyzing the main dimension of the specimen cross sections reported in Fig. 14.

From Fig. 15, it is evident that, the welds made by tools P5-0 and P5-30 ($d = 5$ mm and $D = 10$ mm) are characterized by the highest specific strength. These welds showed a specific shear strength of 25 and 20 N/mm^2, respectively, while the welds made by larger tools were characterized by specific shear strength ranging between 7 and 10 N/mm^2. In addition, since the taper angle involves a lower welded area, the weld made by the cylindrical pin P5-0 was characterized by higher specific strength as compared to that made by the conical pin P5-30.

For the welds made by tools P5-0 and P5-30, it was possible to calculate the shear stress since they failed by pure shearing mode. In these welds, the shear strength, calculated by the ratio of F_r/A_{weld}, reached 31 and 28 MPa, respectively. Using von Mises criterion, the shear yield strength τ_s of a material is given by the yield strength of the material measured by tensile

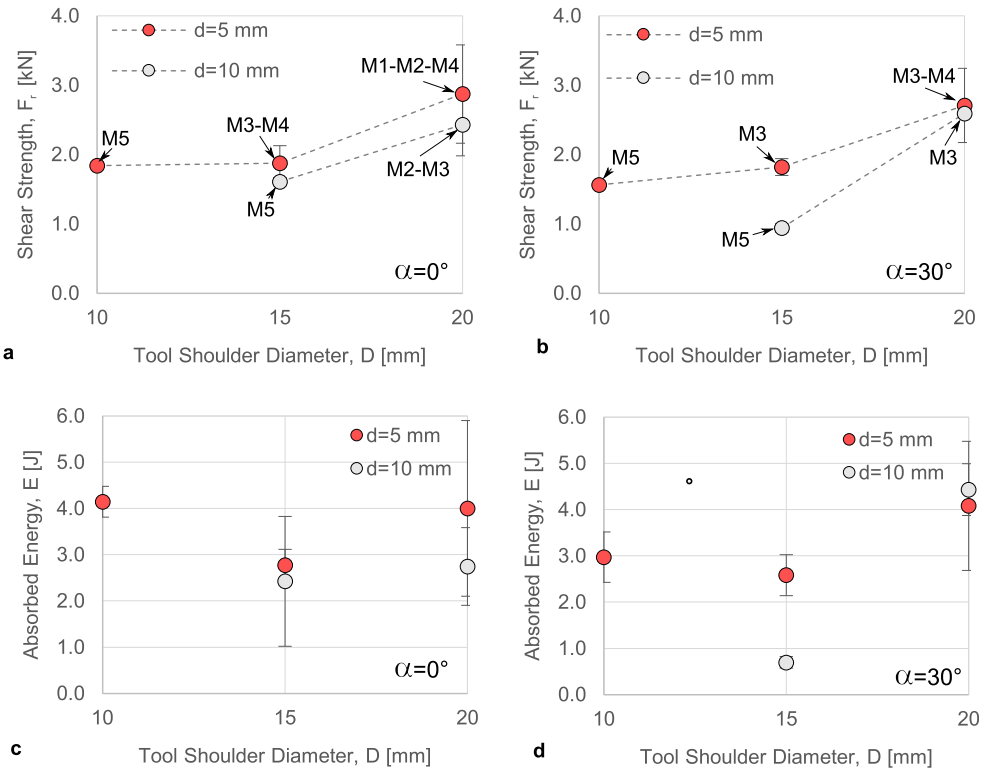

Fig. 13 Effect of the tool pin diameter and shoulder diameter on the shear strength of the welds (**a**, **b**) and on the energy absorbed during the shear test (**c**, **d**)

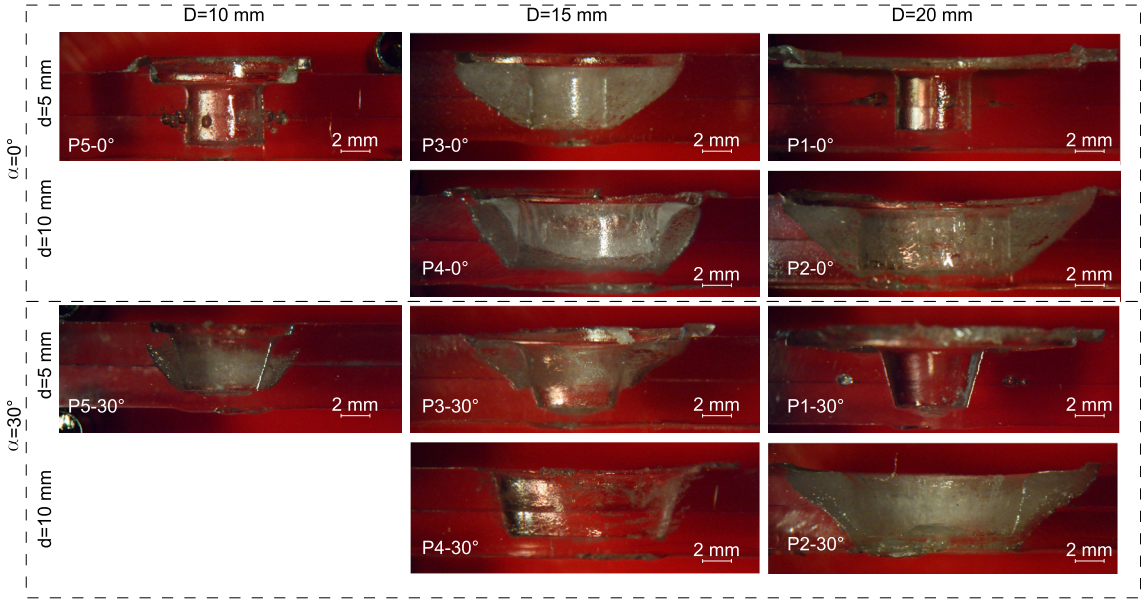

Fig. 14 Cross section of welds performed with different tools

test σ_s divided by the square root of 3: $\tau_s = \sigma_s/\sqrt{3} = 60/1.732 = 34.6$ MPa. Thus, the shear strength of the welds are 88 and 80 % of the shear yield strength of the base material.

4 Conclusions

The present work investigated the main fracture mechanisms developing while testing friction spot stir welds of polymeric materials. The characteristic dimensions of the weld affecting the mechanical behavior of the welds have been identified. The influence of the tool geometry on the morphological and mechanical behavior of the welds was clarified. Sectioned samples were also prepared to understand how the fracture developed and propagated in the welds. The main results are reported as follows:

- Although the high toughness of the polycarbonate material, both brittle and ductile fracture modes were found on FSS welds during single lap shear tests.
- The analysis of the morphology of the weld and the identification of the critical weld areas allowed understanding the influence of the tool geometry on the fracture modes.
- The influence of the plunging depth on the fracture mode and shear strength was clarified. Low values of plunging depth facilitated the separation of the stirred zone from the lower sheet since the small interface area. The increase in the plunging depth results in the increase of this area with increase of the shear strength. Excessive increase of the plunging depth may result in decreasing the weld strength since separation of the stirred zone from the upper sheet is more likely to occur.
- The shear strength of the welds increases with the shoulder diameter (D) and reduces with the pin diameter (d). The taper angle of the tool pin influences the shear strength only for tools with small values of D-d.
- In the welds made by the larger tool shoulder ($D = 20$ mm), different fracture modes may develop (while using the same tool) leading to a high uncertainty of the mechanical behavior of such welds.

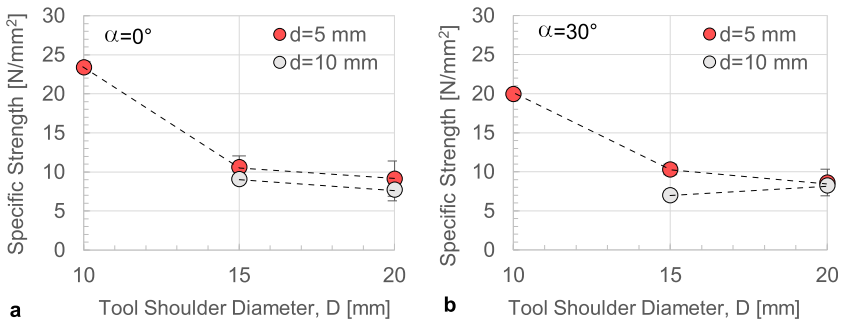

Fig. 15 Effect of process parameters on the specific strength of the welds

- The specific strength is highly influenced by the geometry of the tool. Indeed, it assumes the highest values 25 and 20 N/mm^2 for tools P5-0 and P5-30. These welds were also characterized by high energy absorption and high behavior repeatability. On the other hand, the specific strength dramatically reduces while using larger tools, whereas the specific strength is comprised between 7 and 10 N/mm^2.

Acknowledgments The authors would also like to thank Mr. G. Organtini (DIIIE—University of L'Aquila) for the contribution during the setup and conduction of the experimental tests. The authors would also like to thank Eng. S. Genna from the University of Naples (CIRTIBBS) for his support during fractography analysis.

References

1. Liu FC, Liao J, Nakata K (2014) Joining of metal to plastic using friction lap welding. Mater Des 54:236–244
2. Yusof F, Muhamad M, Moshwan R, Jamaludin M, Miyashita Y (2016) Effect of surface states on joining mechanisms and mechanical properties of aluminum alloy (A5052) and polyethylene terephthalate (PET) by dissimilar friction spot welding. Metals 6(5): 101
3. Junior WS, Handge UA, dos Santos JF, Abetz V, Amancio-Filho ST (2014) Feasibility study of friction spot welding of dissimilar single-lap joint between poly(methyl methacrylate) and poly(methyl methacrylate)-SiO2 nanocomposite. Mater Des 64: 246–250
4. Junior WS, Emmler T, Abetz C, Handge UA, dos Santos JF, Amancio-Filho ST, Abetz V (2014) Friction spot welding of PMMA with PMMA/silica and PMMA/silica-g-PMMA nanocomposites functionalized via ATRP. Polymer 55(20):5146–5159
5. Goushegir SM, dos Santos JF, Amancio-Filho ST (2014) Friction spot joining of aluminum AA2024/carbon-fiber reinforced poly(phenylene sulfide) composite single lap joints: microstructure and mechanical performance. Mater Des 54:196–206
6. Dashatan SH, Azdast T, Ahmadi SR, Bagheri A (2013) Friction stir spot welding of dissimilar polymethyl methacrylate and acrylonitrile butadiene styrene sheets. Mater Des 45:135–141
7. Oliveira PHF, Amancio-Filho ST, dos Santos JF, Hage E (2010) Preliminary study on the feasibility of friction spot welding in PMMA. Mater Lett 64(19):2098–2101
8. Esteves JV, Goushegir SM, dos Santos JF, Canto LB, Hage E, Amancio-Filho ST (2015) Friction spot joining of aluminum AA6181-T4 and carbon fiber-reinforced poly(phenylene sulfide): effects of process parameters on the microstructure and mechanical strength. Mater Des 66:437–445
9. Abibe AB, Sônego M, dos Santos JF, Canto LB, Amancio-Filho ST (2016) On the feasibility of a friction-based staking joining method for polymer–metal hybrid structures. Mater Des 92:632–642
10. Abibe AB, Amancio-Filho ST, dos Santos JF, Hage E (2013) Mechanical and failure behaviour of hybrid polymer–metal staked joints. Mater Des 46:338–347
11. Gao J, Li C, Shilpakar U, Shen Y (2016) Microstructure and tensile properties of dissimilar submerged friction stir welds between HDPE and ABS sheets. Int J Adv Manuf Technol
12. Vijendra B, Sharma A (2015) Induction heated tool assisted friction-stir welding (i-FSW): a novel hybrid process for joining of thermoplastics. J Manuf Process 20:234–244
13. Gao J, Li C, Shilpakar U, Shen Y (2015) Improvements of mechanical properties in dissimilar joints of HDPE and ABS via carbon nanotubes during friction stir welding process. Mater Des 86:289–296
14. Bilici MK, Yukler AI (2012) Effects of welding parameters on friction stir spot welding of high density polyethylene sheets. Mater Des 33:545–550
15. Lambiase F, Paoletti A, Di Ilio A (2016) Effect of tool geometry on loads developing in friction stir spot welds of polycarbonate sheets. Int J Adv Manuf Technol
16. Paoletti A, Lambiase F, Di Ilio A (2016) Analysis of forces and temperatures in friction spot stir welding of thermoplastic polymers. Int J Adv Manuf Technol 83(5–8):1395–1407
17. Paoletti A, Lambiase F, Di Ilio A (2015) Optimization of friction stir welding of thermoplastics. Proc CIRP 33:563–568
18. Lambiase F, Paoletti A, Di Ilio A (2015) Mechanical behaviour of friction stir spot welds of polycarbonate sheets. Int J Adv Manuf Technol 80(1):301–314
19. Hoseinlaghab S, Mirjavadi SS, Sadeghian N, Jalili I, Azarbarmas M, Besharati Givi MK (2015) Influences of welding parameters on the quality and creep properties of friction stir welded polyethylene plates. Mater Des 67:369–378
20. D'Urso G (2015) Thermo-mechanical characterization of friction stir spot welded AA6060 sheets: experimental and FEM analysis. J Manuf Process 17:108–119
21. Mostafapour A, Azarsa E (2012) A study on the role of processing parameters in joining polyethylene sheets via heat assisted friction stir welding: investigating microstructure, tensile and flexural properties. Int J Phys Sci 7 (4)
22. Bozkurt Y (2012) The optimization of friction stir welding process parameters to achieve maximum tensile strength in polyethylene sheets. Mater Des 35:440–445
23. Bilici MK, Yükler Aİ (2012) Influence of tool geometry and process parameters on macrostructure and static strength in friction stir spot welded polyethylene sheets. Mater Des 33:145–152
24. Pirizadeh M, Azdast T, Rash Ahmadi S, Mamaghani Shishavan S, Bagheri A (2014) Friction stir welding of thermoplastics using a newly designed tool. Mater Des 54:342–347
25. Mendes N, Neto P, Simão MA, Loureiro A, Pires JN (2014) A novel friction stir welding robotic platform: welding polymeric materials. Int J Adv Manuf Technol
26. Mendes N, Loureiro A, Martins C, Neto P, Pires JN (2014) Morphology and strength of acrylonitrile butadiene styrene welds performed by robotic friction stir welding. Mater Des 64:81–90
27. Mendes N, Loureiro A, Martins C, Neto P, Pires JN (2014) Effect of friction stir welding parameters on morphology and strength of acrylonitrile butadiene styrene plate welds. Mater Des 58:457–464
28. Simões F, Rodrigues DM (2014) Material flow and thermo-mechanical conditions during friction stir welding of polymers: literature review, experimental results and empirical analysis. Mater Des 59:344–351
29. Bagheri A, Azdast T, Doniavi A (2013) An experimental study on mechanical properties of friction stir welded ABS sheets. Mater Des 43:402–409
30. M. Husain I, K. Salim R, Azdast T, Hasanifard S, M. Shishavan S, Eungkee Lee R (2015) Mechanical properties of friction-stir-welded polyamide sheets. Int J Mech Mater Eng 10 (1)
31. Gonçalves J, dos Santos JF, Canto LB, Amancio-Filho ST (2015) Friction spot welding of carbon fiber-reinforced polyamide 66 laminate. Mater Lett 159:506–509
32. Panneerselvam K, Lenin K (2014) Joining of Nylon 6 plate by friction stir welding process using threaded pin profile. Mater Des 53:302–307
33. Bilici MK (2012) Application of Taguchi approach to optimize friction stir spot welding parameters of polypropylene. Mater Des 35:113–119

34. Payganeh GH, Mostafa Arab NB, Dadgar Asl Y, Ghasemi FA, Saeidi Boroujeni M (2011) Effects of friction stir welding process parameters on appearance and strength of polypropylene composite welds. Int J Phys Sci 6(19):4595–4601
35. Bilici MK (2012) Effect of tool geometry on friction stir spot welding of polypropylene sheets. Express Polym Lett 6(10):805–813
36. Memduh K (2012) Friction stir spot welding parameters for polypropylene sheets. Sci Res Essays 7 (8)
37. Ahmadi H, Arab NBM, Ghasemi FA, Farsani RE (2012) Influence of pin profile on quality of friction stir lap welds in carbon fiber reinforced polypropylene composite. Int J Mech Appl 2(3):24–28
38. Sadeghian N, Besharati Givi MK (2015) Experimental optimization of the mechanical properties of friction stir welded acrylonitrile butadiene styrene sheets. Mater Des 67:145–153
39. Bilici MK, Yükler Aİ, Kurtulmuş M (2011) The optimization of welding parameters for friction stir spot welding of high density polyethylene sheets. Mater Des 32(7):4074–4079
40. Azarsa E, Mostafapour Asl A, Tavakolkhah V (2012) Effect of process parameters and tool coating on mechanical properties and microstructure of heat assisted friction stir welded polyethylene sheets. Adv Mater Res 445:765–770
41. Eslami S, Ramos T, Tavares PJ, Moreira PMGP (2015) Effect of friction stir welding parameters with newly developed tool for lap joint of dissimilar polymers. Proc Eng 114:199–207
42. Paoletti A, Lambiase F, Di Ilio A (2016) Analysis of forces and temperatures in friction spot stir welding of thermoplastic polymers. Int J Adv Manuf Technol